



PB99-147399

**DOT/FAA/AR-98/36**

Office of Aviation Research  
Washington, D.C. 20591

# **Comparison of Boundary Correction Factor Solutions for Two Symmetric Cracks in a Straight-Shank Hole**

John G. Bakuckas, Jr.  
Federal Aviation Administration  
Airport and Aircraft Safety  
Research and Development Division  
William J. Hughes Technical Center  
Atlantic City International Airport, NJ 08405

April 1999

Final Report

This document is available to the U.S. public  
through the National Technical Information  
Service (NTIS), Springfield, Virginia 22161.



**U.S. Department of Transportation  
Federal Aviation Administration**


REPRODUCED BY:  
U.S. Department of Commerce  
National Technical Information Service  
Springfield, Virginia 22161

**NTIS**

## NOTICE

This document is disseminated under the sponsorship of the U.S. Department of Transportation in the interest of information exchange. The United States Government assumes no liability for the contents or use thereof. The United States Government does not endorse products or manufacturers. Trade or manufacturer's names appear herein solely because they are considered essential to the objective of this report. This document does not constitute FAA certification policy. Consult your local FAA aircraft certification office as to its use.

This report is available at the Federal Aviation Administration William J. Hughes Technical Center's Full-Text Technical Reports page:  
[www.tc.faa.gov/its/act141/reportpage.html](http://www.tc.faa.gov/its/act141/reportpage.html) in Adobe Acrobat portable document format (PDF).

1. Report No. DOT/FAA/AR-98/36	2. Government Accession No.	3. Recipient's Catalog No.	
4. Title and Subtitle  COMPARISON OF BOUNDARY CORRECTION FACTOR SOLUTIONS FOR TWO SYMMETRIC CRACKS IN A STRAIGHT-SHANK HOLE		5. Report Date April 1999	
		6. Performing Organization Code	
7. Author(s) John G. Bakuckas, Jr.		8. Performing Organization Report No.	
9. Performing Organization Name and Address Federal Aviation Administration Airport and Aircraft Safety Research and Development Division William J. Hughes Technical Center Atlantic City International Airport, NJ 08405		 PB99-147399	
		11. Contract or Grant No.	
12. Sponsoring Agency Name and Address U.S. Department of Transportation Federal Aviation Administration Office of Aviation Research Washington, DC 20591		13. Type of Report and Period Covered Final Report	
		14. Sponsoring Agency Code AAR-431	
15. Supplementary Notes			
16. Abstract  This report compares the mode I boundary correction factor solutions for two symmetric elliptical cracks emanating from a straight-shank hole. A variety of methods were used to generate the solutions. A global-intermediate-local (GIL) hierarchical approach was developed using the finite element method (FEM). Comparisons were made with the following methods: the FEM with the equivalent domain integral, semiempirical boundary correction factor equations, the finite element alternating method, the boundary element method with the crack opening displacement approach, the boundary element method using special crack-tip elements, and the three-dimensional weight function method. The boundary correction factor solutions were within a band of $\pm 3\%$ of the average solution.			
17. Key Words Stress-intensity factor; global, local, intermediate model; Finite element method, three-dimensional		18. Distribution Statement This document is available to the public through the National Technical Information Service (NTIS), Springfield, Virginia 22161.	
19. Security Classif. (of this report) Unclassified	20. Security Classif. (of this page) Unclassified	21. No. of Pages 22	22. Price



## PREFACE

The author would like to thank the investigators listed in table 1 for their participation in this study. In addition, the discussion and participation of Dr. Anis Rahman, Drexel University, in developing the GIL approach is gratefully acknowledged.

PROTECTED UNDER INTERNATIONAL COPYRIGHT  
ALL RIGHTS RESERVED.  
NATIONAL TECHNICAL INFORMATION SERVICE  
U.S. DEPARTMENT OF COMMERCE



## TABLE OF CONTENTS

	Page
EXECUTIVE SUMMARY	vii
INTRODUCTION	1
CONFIGURATION AND LOADING	3
DEFINITION OF STRESS-INTENSITY FACTOR	3
GLOBAL-INTERMEDIATE-LOCAL HIERARCHICAL APPROACH	3
RESULTS AND DISCUSSION	4
Convergence Studies	4
Conventional Versus Singularity	5
Solution Comparisons	5
CONCLUDING REMARKS	6
REFERENCES	6

## LIST OF FIGURES

Figure		Page
1	Problem Description	10
2	Global-Intermediate-Local Hierarchical Approach	10
3	Convergence Study Comparison of Results From Two Meshes of Local Model	11
4	Comparison of Results Using Conventional and Singularity Elements	11
5	Comparison of Results From All Solution Methods	12

## LIST OF TABLES

Table		Page
1	Study Participants and Methods Used	12
2	Boundary Correction Factors From Three Meshes of Local Model	13
3	Boundary Correction Factors From a Variety of Approaches	14
4	Parameters Used in Semiempirical Equation	15



## EXECUTIVE SUMMARY

This report compares the mode I boundary correction factor solutions for two symmetric elliptical cracks emanating from a straight-shank hole. A variety of methods were used to generate the solutions. A global-intermediate-local (GIL) hierarchical approach was developed using the finite element method (FEM). Comparisons were made with the following methods: the FEM with the equivalent domain integral, semiempirical boundary correction factor equations, the finite element alternating method, the boundary element method with the crack opening displacement approach, the boundary element method using special crack-tip elements, and the three-dimensional weight function method. The boundary correction factor solutions were within a band of  $\pm 3\%$  of the average solution.



## INTRODUCTION

Accurate stress-intensity factor (SIF) solutions are required to conduct thorough damage tolerance analyses of structures containing cracks. Exact closed form SIF solutions for cracks in three-dimensional solids are often lacking for complex configurations; therefore, approximate solutions must be used. Over the past two decades, considerable effort has been placed on developing computationally efficient methods which provide highly accurate SIF solutions for cracks in three-dimensional bodies. A review of methods for the analysis of cracks in three-dimensional solids was provided in reference 1. Various methods have been used to obtain SIF solution for surface and corner cracks in plates including the conventional finite element method (FEM) [2-8], the finite element alternating method (FEAM) [9-12], the boundary element method (BEM) [13-15], and the three-dimensional weight function method (WFM) [16-19]. With advances in pre- and postprocessors, computer hardware, and improvements in equation solvers, time savings are being realized in both geometry development and analysis of complex models. With computational tools in place, SIF solutions required for damage tolerance assessments of cracked complex structures can be obtained.

Two steps are typically used to obtain SIF solutions. First, the stress and displacement fields for the structure under the prescribed loading conditions are calculated. Second, the SIF solutions are extracted from the governing stress and displacement fields. One of the most commonly used approaches to determine SIF solutions is the FEM. Several techniques have been developed using FEM to approximate SIF solutions for cracks in three-dimensional solids including the crack opening displacement (COD) method [20], the virtual crack extension (VCT) method [21-22], the virtual crack closure technique (VCCT) [23], and the J-integral method using the equivalent domain integral method (DIM) [8,9,24,25]. Stress-intensity factor equations have also been obtained by fitting empirical equations to some of the SIF solutions obtained by finite element analyses [26].

The FEAM [9-11] is an iterative approach alternating between a finite element analysis of the uncracked finite body and an analytical solution of a crack subjected to traction forces in an infinite medium. The FEAM is a computationally efficient approach to obtain three-dimensional SIF solutions. Since the SIF is calculated using the analytical solution, the crack front does not need to be modeled explicitly in the finite element analysis. Only the stress concentrations due to the geometry of the configuration, i.e., holes and cutouts, need to be accurately modeled. Thus, a relatively coarse mesh having a simple configuration of finite elements can be used in the FEAM compared with conventional FEM used in fracture problems.

In the three-dimensional BEM, only the surface of the body needs to be modeled. Thus, a model may be built relatively quickly compared with conventional FEM. Two programs that use the BEM have been recently developed for fracture mechanics studies. The first, FRacture ANalysis Code in 3-Dimensions (FRANC3D), is a special purpose fracture mechanics and crack growth simulation program which integrates a graphics user interface pre- and postprocessor, a boundary element solver for three-dimensional solids, and a generalized shell analysis solver [27-30]. SIF solutions are obtained using the COD method. Plane strain assumptions are used in the calculation. The second program, Fracture Analysis by Distributed Dislocations in 3-Dimensions (FADD3D) is a weakly singular, symmetric Galerkin BEM for the analysis of linearly elastic,

isotropic, three-dimensional solids containing fractures [31,32]. An important aspect of the numerical implementation in FADD3D is the use of a special crack-tip element which has degrees of freedom along the crack front that correspond to the three modes of stress-intensity factors which are solved for directly. The method is applicable to a wide class of fracture problems and has proven to provide highly accurate SIF solutions using relatively coarse meshes.

The WFM [16-19] is an efficient and accurate technique for determining three-dimensional SIF solutions. Using this approach a three-dimensional body is decomposed into thin slices in the thickness and width directions. Each slice is assumed to be in a state of generalized plane stress. The three-dimensional effect is accounted for by forces acting on the crack surface due to shear loading between slices and the restraining effect of the uncracked area on the cracked slices.

Several investigators have used hierarchical level approaches to study cracks in fuselage shell structure [33-37]. The advantage of a hierarchical level approach is that model development and analysis efforts are simplified by breaking a problem down to manageable levels of relative scale and detail. Boundary conditions at each level of analysis are passed onto subsequent analysis levels. At the highest level, a global analysis is conducted using known prescribed boundary conditions applied to the fuselage which was typically idealized using shell elements to model the skin and beam elements to model the substructure (frames and stringers). The purpose of the global analysis is to obtain accurate stress and displacement fields in the area of interest resulting from the known boundary conditions. These stress and displacement fields are used as boundary conditions in the next level, a submodel that is a dimensional subset of the previous level and is modeled with a more refined mesh with higher substructure detail. Higher order shell elements are typically used to model the substructure. At the final level, a local analysis is conducted on a highly refined mesh focused at the crack tip to determine the SIF solutions. The number of levels used in a hierarchical level approach depends on the complexity and size of the problem being analyzed. A two-level global-local approach was sufficient to obtain accurate results for large cracks terminating in the skin bay region of fuselage structure [36, 37] whereas a three-level global-intermediate-local approach was required to analyze small cracks emanating from rivet holes in fuselage lap joint [33].

In this study, a three-level global-intermediate-local (GIL) hierarchical approach was developed using FEM for the fracture mechanics analysis of cracks in three-dimensional solids. Verification studies of the GIL approach were conducted using a problem consisting of two symmetric cracks emanating from a straight-shank hole under remote tension. First, convergence studies were done to determine the level of mesh refinement needed for the global, intermediate, and local models. Next, the use of conventional and singularity elements in the local model was assessed. The solution obtained from the GIL approach was verified and compared with the solutions obtained by several investigators using a variety of methods including the equivalent domain integral method (DIM), semiempirical SIF equations, the FEAM, the BEM with the crack opening displacement approach (FRANC3D), the BEM with special crack-tip elements (FADD3D), and the three-dimensional Weight Function Method (WFM). Table 1 lists the methods that were compared and the participants who provided the solutions for each method.

## CONFIGURATION AND LOADING

The problem analyzed in this study consists of a pair of symmetric elliptical cracks emanating from a straight-shank hole in a plate under far-field tension, figure 1. The half height of the plate ( $H$ ) and half width ( $W$ ) were chosen to be large enough to have a negligible effect on the stress-intensity factors ( $H/W = 2$ ) and the ratio of the straight-shank hole radius to plate width ( $R/W$ ) was 0.2. The ratio of hole radius to thickness ( $R/t$ ) was 2. The plate has a modulus of elasticity,  $E = 1$  psi, and Poisson's ratio,  $\nu = 0.3$ .

A symmetrical elliptical corner crack configuration was analyzed with a crack depth to plate thickness ratio ( $a/t$ ) of 0.2 and a crack depth to crack length ratio ( $a/c$ ) of 0.8. A remote tension load was applied with a constant stress,  $S_t = 1.0$  unit force per unit area.

## DEFINITION OF STRESS-INTENSITY FACTOR

The mode I stress-intensity factor ( $K_I$ ) at any location along the crack front under tensile loading is given as

$$K_I = S_t \sqrt{\frac{\pi a}{Q}} F_t \left( \frac{a}{t}, \frac{a}{c}, \frac{R}{t}, \varphi \right) \quad (1)$$

where the boundary correction factor,  $F_t$  (tensile), is calculated along the crack front as a function of the parametric angle. The crack dimensions and parametric angle,  $\varphi$ , are defined in figure 1. The parametric angle is the angle measured with reference to the circle contained within the ellipse defining the crack front. The angle,  $\varphi$ , is measured from the surface of the plate to the boundary of the straight-shank hole. The shape factor for an ellipse,  $Q$ , is the square of the complete elliptic integral of the second kind [2]

$$\left. \begin{aligned} Q &= 1 + 1.464 \left( \frac{a}{c} \right)^{1.65} & \text{for } \frac{a}{c} \leq 1 \\ Q &= 1 + 1.464 \left( \frac{c}{a} \right)^{1.65} & \text{for } \frac{a}{c} > 1 \end{aligned} \right\} \quad (2)$$

## GLOBAL-INTERMEDIATE-LOCAL HIERARCHICAL APPROACH

In the hierarchical approaches, model development and analysis efforts are simplified by breaking a problem into manageable levels of relative scale and detail. Boundary conditions at each level of analysis are passed onto subsequent analysis levels. A three-level global-intermediate-local (GIL) hierarchical finite element approach was used in this study to obtain the SIF solutions for the problem as illustrated in figure 2. The commercially available finite element program ABAQUS 5.6 [38] was used for the analysis. In the first step (global level) of the GIL approach, an analysis of the plate subjected to the prescribed loading conditions was conducted. The crack was modeled in the global level using conventional elements. A typical mesh for the global level is shown in figure 2. Due to symmetry in the geometry and loading, one quadrant of the plate was modeled. A typical mesh for the global model contained 1312

twenty-noded brick elements. Along the top edge, a 1-psi stress was applied. Symmetry boundary conditions were applied as indicated in the figure.

In the second step (intermediate level), an analysis was conducted in the high stress gradient region near the straight-shank hole. A refined mesh, shown in figure 2, of the region near the hole was used to accurately capture the stress concentrations. The crack region was modeled in the intermediate level using conventional elements. A typical mesh for the intermediate model consisted of 5764 twenty-noded brick elements. Symmetry boundary conditions were applied to the crack plane. The boundary conditions for the intermediate model were taken from the global model using the submodelling features in ABAQUS.

In the final step (local level), a local analysis was conducted of a region around the crack front. A highly refined mesh with elements orthogonal to the crack front was used. The length of the elements along the crack front was less than or equal  $a/20$  where  $a$  is the minor crack length of the elliptical crack. Two types of meshes were used as shown in figure 2. The first mesh, containing only conventional elements, consisted of 1728 twenty-noded brick elements. The second mesh, consisting of 1152 twenty-noded brick elements, contained a ring of singularity elements surrounding the crack front. The singularity elements are twenty-noded isoparametric brick elements with one side collapsed along the crack front and with the midside nodes on the element sides adjacent to the collapsed side shifted to the quarter point to obtain the  $1/\sqrt{r}$  singularity. In both local meshes, symmetry boundary conditions were applied on the crack plane. The intermediate model using the submodelling features in ABAQUS provided displacement boundary conditions along the perimeter of the local model.

The J-integral was calculated along the crack front using the equivalent domain integral (EDI) method. For cases where there is no mixed mode fracture and assuming a plane strain elastic material response, the mode I SIF at any point along the crack front can be calculated from the J-integral as

$$K_I = \sqrt{\frac{JE}{1-\nu^2}} \quad (3)$$

## RESULTS AND DISCUSSION

### CONVERGENCE STUDIES.

Convergence studies were done to determine the level of mesh refinement needed for each of the global, intermediate, and local models. Typical results for the convergence study are shown in figure 3 and table 2. Results are presented in terms of the variation of the boundary correction factor,  $F_b$ , as a function of the parametric angle,  $\phi$ , for two meshes of the local model. The first mesh, Mesh A, consisted of 216 elements with 12 elements along the crack front. The second mesh, Mesh B, was much more refined consisting of 1728 elements with 24 elements along the crack front. Both meshes used conventional elements. As shown, the results obtained using the different mesh refinements differed by less than 0.8% indicating a converged solution was obtained.

## CONVENTIONAL VERSUS SINGULARITY.

The use of conventional and singularity elements to model the crack front in the local model was compared. The boundary correction factor,  $F_t$ , calculated using conventional and singularity elements as a function of the parametric angle,  $\phi$ , is shown in figure 4 and table 2. The crack front was modeled using conventional elements (Mesh B) and singularity elements (Mesh C). As shown in figure 4, excellent agreement was obtained where the results from the two crack front meshes differed by less than 0.6%.

Modeling the crack front using singularity elements has the advantage of capturing the square root singularity and obtaining accurate near-field stresses and displacements. However, the process of forming a singularity element from a conventional brick element by collapsing the side nearest the crack front and moving the midside nodes to the quarter point can be an extremely tedious and time consuming task. Modeling the crack front using conventional elements is much easier and the use of conventional elements in fracture mechanics studies is viable provided that the elements are of proper size (approximate length of  $a/20$ ) and are orthogonal to the crack front. When the equivalent domain integral method is used to determine the J-integral, it is not necessary to have extremely accurate stress and displacement fields. As the volume contour around the crack front used in the calculation of the J-integral increases, the influence of the high stress and displacement gradients dissipates.

## SOLUTION COMPARISONS.

The solution obtained from the GIL approach was verified and compared with the solutions obtained by other investigators using the methods listed in table 1. The following methods were used: the FRacture ANalysis Code in 3-Dimensions (FRANC3D) conducted by Cornell University, the three-dimensional Weight Function Method (WFM) conducted by University of South Carolina, the finite element alternating method (FEAM) conducted by Knowledge Systems, Incorporated, the finite element method (FEM) with the equivalent domain integral (DIM) conducted by Northwestern University [7], and the Fracture Analysis by Distributed Dislocation in 3-Dimension (FADD3D) conducted by the University of Texas, Austin. In addition, the semiempirical SIF equation developed at NASA Langely [26] was used in the comparison. For the problem defined in figure 1, the semiempirical equation [26] is given by

$$F_t = \left( M_1 + M_2 \left( \frac{a}{t} \right)^2 + M_3 \left( \frac{a}{t} \right)^4 \right) g_1 g_2 g_3 g_4 f_\phi f_w \quad (4)$$

where the parameters in equation 4 are provided in table 4.

The results of the various methods are shown in figure 5 and table 3 as boundary correction factors along the crack front as a function of the parametric angle,  $\phi$ . Excellent agreement was obtained among the methods listed in table 1 as shown in figure 5. The dashed line indicates the result from the semiempirical equation [26]. Results from the FRANC3D, FEAM, WFM, DIM, FADD3D, and GIL were averaged. The results calculated using the semiempirical SIF equation

were similar to the average solution. All solutions were within a narrow band of  $\pm 3\%$  about the average solution; the  $\pm 3\%$  band is shown by the solid lines in figure 5.

### CONCLUDING REMARKS

A global-intermediate-local (GIL) hierarchical approach was developed using the finite element method (FEM). The objective was to develop and verify the GIL approach by comparing the GIL results to results from various other methods. Using the GIL approach, the boundary correction factors along the crack front were calculated using the equivalent domain integral method. Convergence studies were done to determine the level of mesh refinement needed for each of the global, intermediate, and local models. The use of conventional elements to model crack front provided the same boundary correction factor results as using singularity elements.

For the problem of two symmetric cracks emanating from a straight-shank hole under remote tension, a comparison was made with a variety of other methods: finite element method (FEM) with the equivalent domain integral method (DIM), semiempirical equations, the finite element alternating method (FEAM), boundary element method (BEM) with the crack opening displacement approach (FRANC3D), the BEM using special crack-tip elements (FADD3D), and the three-dimensional Weight Function Method (WFM). Results for all the methods were in excellent agreement and fell within a band of  $\pm 3\%$  of the average of all the solutions. These results verified the GIL approach developed in the current study.

These results also show that there are a variety of computational methods that can be used to calculate accurate boundary correction factor solutions for cracks in three-dimensional solids. It should be pointed out, however, that these are all sophisticated, complex methods that require a knowledgeable user. Those methods that use a mesh (whether boundary element or finite element methods) also require convergence studies to insure that the mesh is refinement sufficient to obtain the desired accuracy.

### REFERENCES

1. Raju, I. S. and Newman, J. C. Jr., "Methods for Analysis of Cracks in Three-Dimensional Solids," *NASA Technical Memorandum 86266*, July 1984.
2. Raju, I. S. and Newman, J. C., Jr., "Stress-Intensity Factors for a Wide Range of Semi-Elliptical Surface Cracks in Finite-Thickness Plates," *Engineering Fracture Mechanics*, Vol. 11, No. 4, 1979, pp. 817-829.
3. Newman, J. C., Jr. and Raju, I. S., "Analyses of Surface Cracks in Finite Plates Under Tension and Bending Loads," *NASA TP-1578*, 1979.
4. Pickard, A. C., "Stress-Intensity Factors for Cracks With Circular and Elliptic Crack Fronts - Determined by 3D Finite Element Methods," PNR-90035, Rolls Royce Limited, May 1980.



5. Raju, I. S. and Newman, J. C., Jr., "Stress-Intensity Factors for Corner Cracks in Rectangular Bars," *Fracture Mechanics: Nineteenth Symposium, ASTM STP 969*, T. A. Cruse (ed.), American Society for Testing and Materials, 1988, pp. 43-55.
6. Tan, P. W., Raju, I. S., Shivakumar, K. N., and Newman, J. C., Jr., "Evaluation of Finite-Element Models and Stress-Intensity Factors for Surface Cracks Emanating from Stress Concentrations," *Surface-Crack Growth: Models, Experiments, and Structures, ASTM STP 1060*, American Society for Testing and Materials, 1990, pp. 34-48.
7. Gosz, M. and Moran, B., "Stress-Intensity Factors Along Three-Dimensional Elliptical Crack Fronts," *DOT Report - DOT/FAA/AR-96/97*, May 1998.
8. Gosz, M. and Moran, B., "Stress-Intensity Factors for Elliptical Cracks Emanating From Countersunk Rivet Holes," *DOT Report - DOT/FAA/AR-95/111*, April 1998.
9. Nishioka, T. and Atluri, S. N., "Analytical Solution for Embedded Elliptical Cracks, and Finite Element-Alternating Method for Elliptical Surface Cracks, Subjected to Arbitrary Loadings," *Engineering Fracture Mechanics*, Vol. 17, 1983, pp. 247-268.
10. Nishioka, T. and Atluri, S. N., "An Alternating Method for Analysis of Surface Flawed Aircraft Structural Components," *AIAA Journal*, Vol. 21, 1983, pp. 749-757.
11. Atluri, S. N. and Nishioka, T., "Computational Methods for Three-Dimensional Problems of Fracture," *Computational Methods in Mechanics of Fracture*, S. N. Atluri (ed.), North Holland, Chapter 7, 1986, pp. 230-287.
12. Tan, P. W., Bigelow, C. A., O'Donoghue, P. E., and Atluri, S. N., "Stress-Intensity Factor Solutions for Cracks at Countersunk Rivet Holes Under Uniaxial Tension," *DOT Report - DOT/FAA/CT-93/68*, February 1994.
13. Cruse, T. A., "Application of Boundary-Integral Equation Method to Three-Dimensional Stress Analysis," *Computer and Structures*, Vol. 3, 1973, pp. 509-527.
14. Cruse, T. A. and Wilson, R. B., "The Use of Singularity Functions in Boundary-Integral Equation Fracture Mechanics Modeling," *Recent Advances in Engineering Sciences, Proceedings of the 14<sup>th</sup> Annual Meeting*, Bethlehem, PA, 1977, pp. 919-924.
15. Heliot, J., Labbens, R. C., and Pellissier-Tanon, A., "Semi-Elliptical Surface Cracks Subjected to Stress Gradients," *Fracture Mechanics, ASTM STP 677*, C.W. Smith (ed.), American Society for Testing and Materials, 1979, pp. 341-364.
16. Zhao, W., Wu, X. R., and Yan, M. G., "Weight Function Method for Three-Dimensional Crack Problems," *Engineering Fracture Mechanics*, Vol. 34, No. 3, 1989, pp. 593-607.
17. Zhao, W. and Wu, X. R., "Stress-Intensity Factor Evaluation by Weight Function for Surface Crack in Edge Notch," *Theoretical and Applied Fracture Mechanics*, Vol. 13, 1990, pp. 225-238.

18. Zhao, W. and Wu, X. R., "Stress-Intensity Factors for Corner Cracks at a Semi-Circular Notch Under Stress Gradients," *Fatigue and Fracture of Engineering Materials and Structures*, Vol. 13, No. 4, 1990, pp. 347-360.
19. Zhao, W., Newman, J. C., Jr., Sutton, M. A., Wu, X. R., and Shivakumar, K. N., "Analysis of Corner Cracks at Hole by a 3-D Weight Function Method with Stresses From Finite Element Method," *NASA Technical Memorandum 110144*, July 1995.
20. Raju, I. S. and Newman, J. C., Jr., "SURF3D: A 3-D Finite Element Program for the Analysis of Surface and Corner Cracks in Solids Subjected to Mode I Loadings," *NASA Technical Memorandum 107710*, February 1993.
21. Parks, D. M., "A Stiffness Derivation Finite Element Technique for Determination of Crack-Tip Stress-Intensity Factors," *International Journal of Fracture*, Vol. 12, 1974, pp. 487-502.
22. Hellen, T. K., "On the Method of Virtual Crack Extensions," *International Journal of Numerical Methods in Engineering*, Vol. 9, No. 1, 1975, pp. 187-208.
23. Shivakumar, K. N., Tan, P. W., and Newman, J. C. Jr., "A Virtual Crack-Closure Technique for Calculating Stress-Intensity Factors for Cracked Three-Dimensional Bodies," *International Journal of Fracture*, Vol. 36, 1988, pp. R43-R50.
24. Nikishkov, G. P. and Atluri, S. N., "Calculation of Fracture Mechanics Parameters for Arbitrary Three-Dimensional Crack by the 'Equivalent Domain Integral' Method," *International Journal of Numerical Methods in Engineering*, Vol. 24, 1987, pp. 1801-1821.
25. Shivakumar, K. N. and Raju, I. S., "An Equivalent Domain Integral Method for Three-Dimensional Mixed-Mode Fracture Problems," *NASA Contractor Report 182021*, August 1991.
26. Newman, J. C., Jr. and Raju, I. S., "Stress-Intensity Factor Equations for Cracks in Three-Dimensional Finite Bodies Subjected to Tension and Bending Loads," *Computational Methods in the Mechanics of Fracture*, S. N. Atluri, ed., Elsevier Science Publishers, 1986, pp. 311-334.
27. Martha, L. F. C. R., "Topological and Geometrical Modeling Approach to Numerical Discretization and Arbitrary Fracture Simulation in Three-Dimensions," Ph.D. Dissertation, Cornell University, Ithaca, NY, 1989.
28. Wawrzynek, P. A., Carter, B. J., Ingraffea, A. R., and Potyondy, D. O., "A Topological Approach to Modeling Arbitrary Crack Propagation in 3D," *DIANA Computational Mechanics '94*, G.M.A. Kusters and M.A.N. Hendriks (eds.), Kluwer Academic Publishers, Netherlands, 1994, pp. 69-84.

29. Wawrzynek, P. A., "Discrete Modelling of Crack Propagation: Theoretical Aspects and Implementation Issues in Two and Three Dimensions," Ph.D. Dissertation, Cornell University, Ithaca, NY, 1991.
30. Martha, L. F., Wawrzynek, P. A., and Ingraffea, A. R., "Arbitrary Crack Representation Using Solid Modeling," *Engineering with Computers*, Vol. 9, 1993, pp. 63-82.
31. S. Li and M.E. Mear, "Singularity-Reduced Integral Equations for Displacement Discontinuities in Three-Dimensional Linear Elastic Media," *International Journal of Fracture*, 1998, in press.
32. S. Li, M.E. Mear, and L. Xiao, "Symmetric Weak-Form Integral Equation Method for Three-Dimensional Fracture Analysis," *Computational Methods Applied Mech. Engrg.*, 151, 1998, pp. 435-459.
33. Starnes, J. H., Britt, V. O., Young, R. D., Rankin, C. C., Shore, C. P., and Bains, J. C., "Nonlinear Analysis of Damaged Stiffened Fuselage Shells Subjected to Combined Loading," *FAA/NASA International Symposium on Advanced Durability and Damage Tolerance, NASA Conference Publication 3274, Part 2*, September 1994, pp. 1045-1075.
34. Zhang, J., Park, J. H., and Atluri, S. N., "Analytical Fatigue Life Estimation of Full-Scale Fuselage Panel," Proceedings of the FAA-NASA Symposium on Continued Airworthiness of Aircraft Structures, *DOT/FAA/AR-97/2, I*, ed. C. A. Bigelow, July 1997, pp. 51-62.
35. Harris, C. H., Newman, J. C., Newman, Jr., Piascik, R. S., and Starnes, J. H., "Analytical Methodology for Predicting Fatigue Damage in Fuselage Structure," Proceedings of the FAA-NASA Symposium on Continued Airworthiness of Aircraft Structures, *DOT/FAA/AR-97/2, I*, ed. C. A. Bigelow, July 1997, pp. 63-88.
36. Bakuckas, J. G., Nguyen, P. V., and Bigelow, C. A., "Bulging Factors for Predicting Residual Strength of Fuselage Panels," *Proceedings of the 19<sup>th</sup> Symposium of the International Committee on Aeronautical Fatigue, ICAF 97*, Edinburgh, United Kingdom 1997, pp. 179-196.
37. Bakuckas, J. G., Nguyen, P. V., and Bigelow, C. A., "Engineering Fracture Parameters for Bulging Cracks in Pressurized Unstiffened Curved Panels," Proceedings of the FAA-NASA Symposium on the Continued Airworthiness of Aircraft Structures, *DOT/FAA/AR-97/2, I*, ed. C. A. Bigelow, July 1997, pp. 239-252.
38. ABAQUS Version 5.6, Hibbitt, Karlsson, and Sorensen (HKS), 1080 Main Street, Pawtucket, RI 02860, USA, 1996.

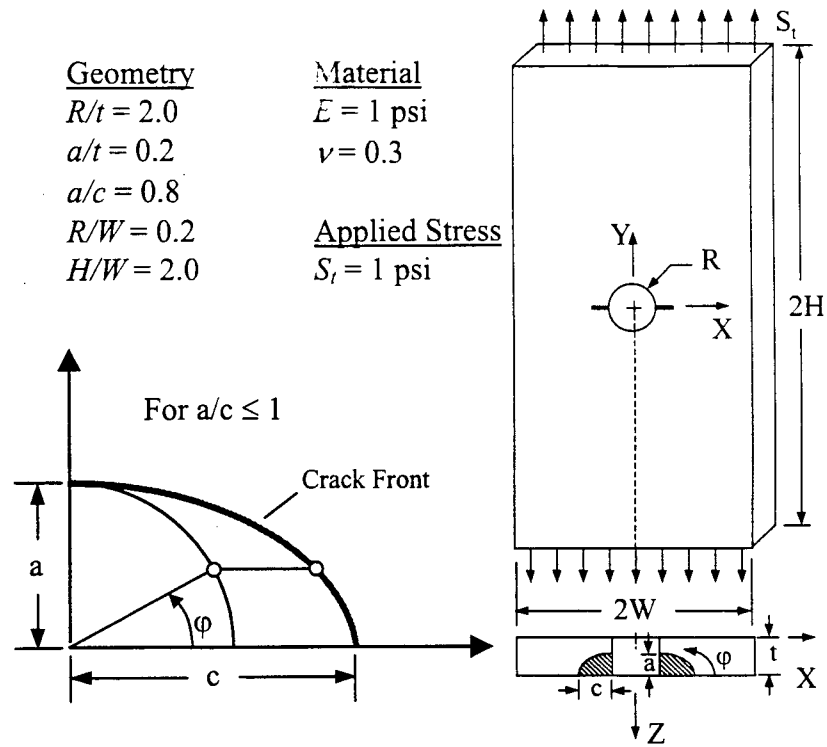


FIGURE 1. PROBLEM DESCRIPTION

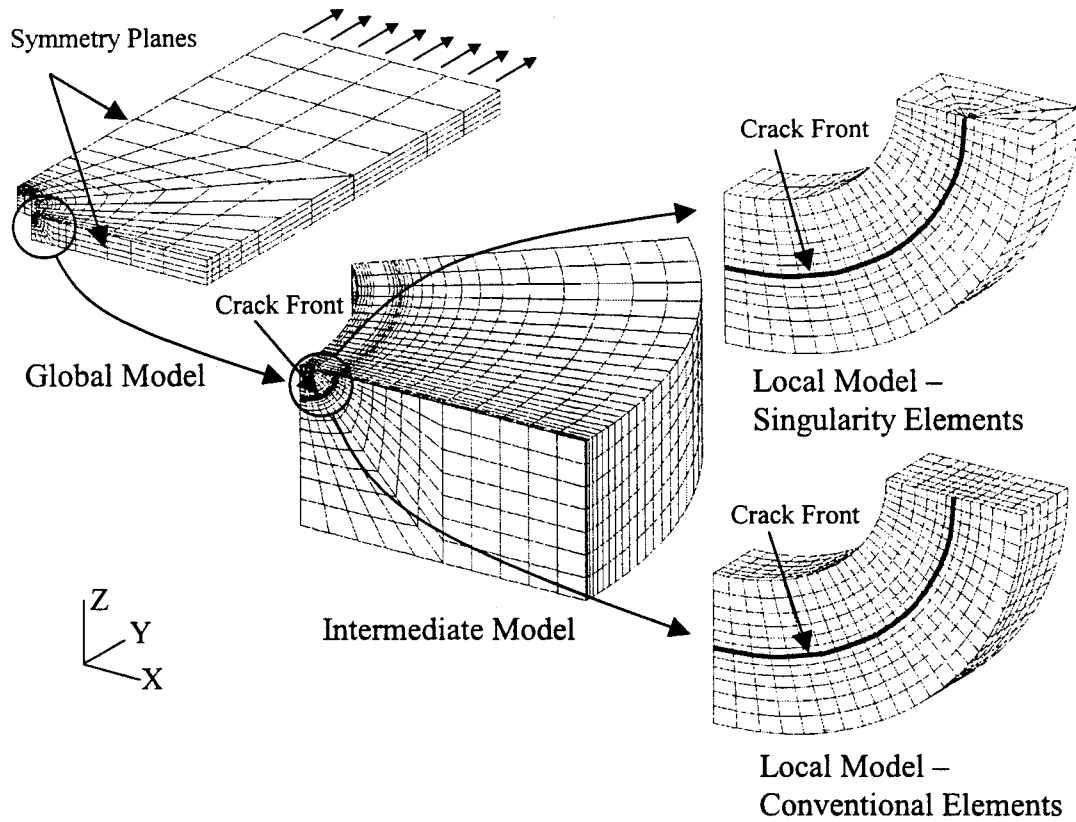


FIGURE 2. GLOBAL-INTERMEDIATE-LOCAL HIERARCHICAL APPROACH

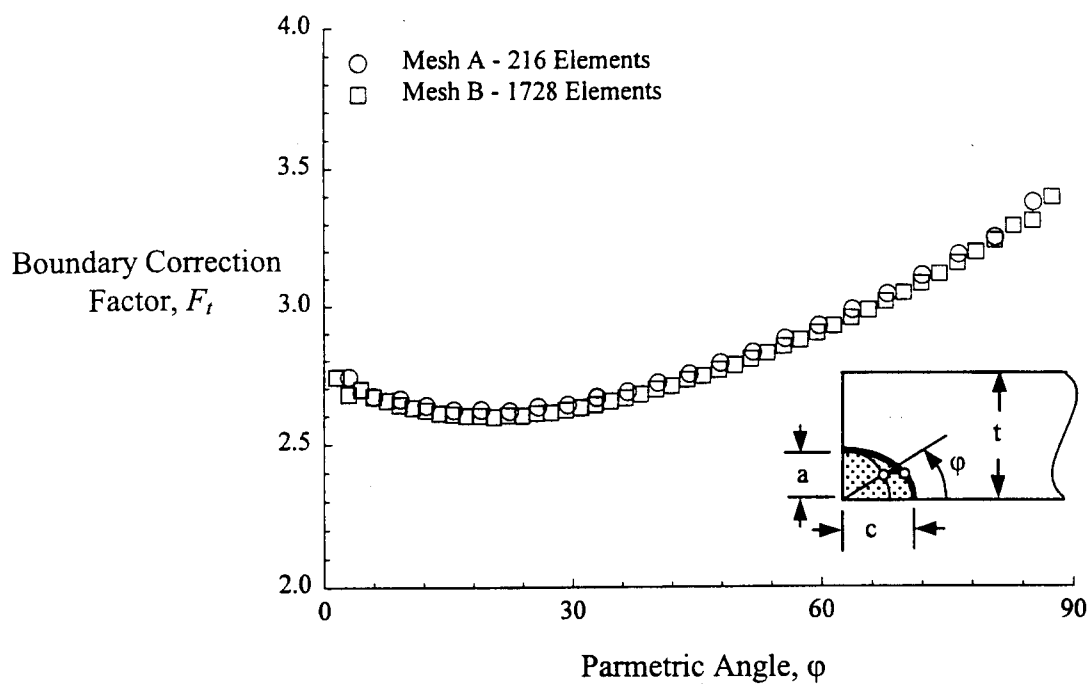


FIGURE 3. CONVERGENCE STUDY COMPARISON OF RESULTS FROM TWO MESHES OF LOCAL MODEL

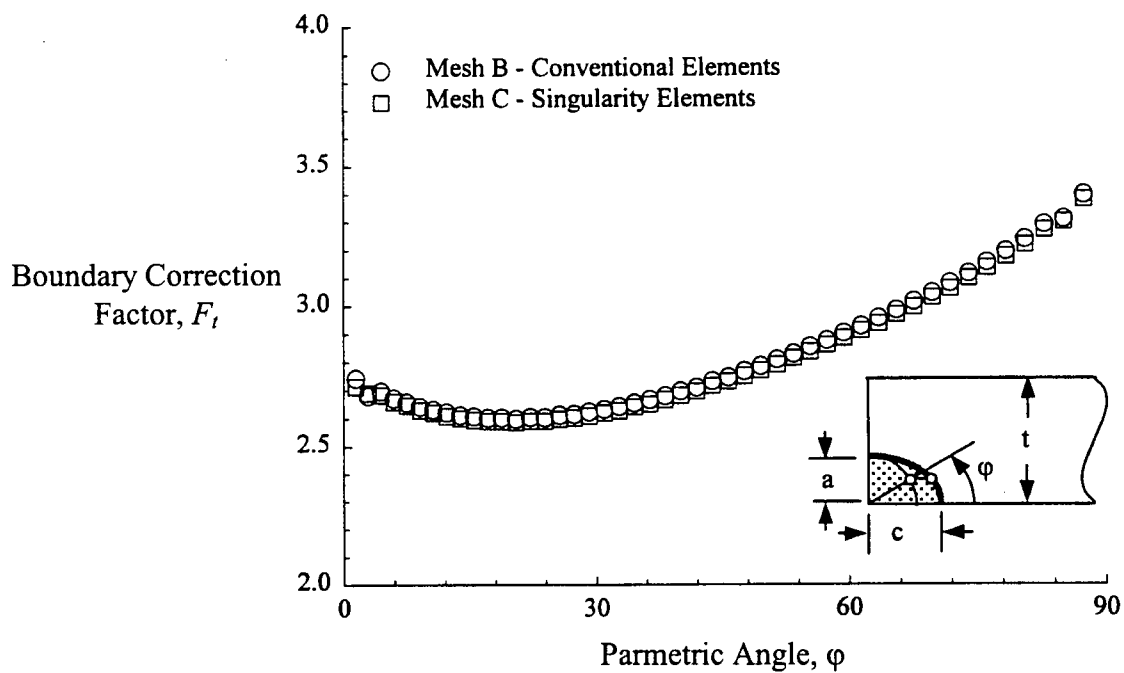


FIGURE 4. COMPARISON OF RESULTS USING CONVENTIONAL AND SINGULARITY ELEMENTS

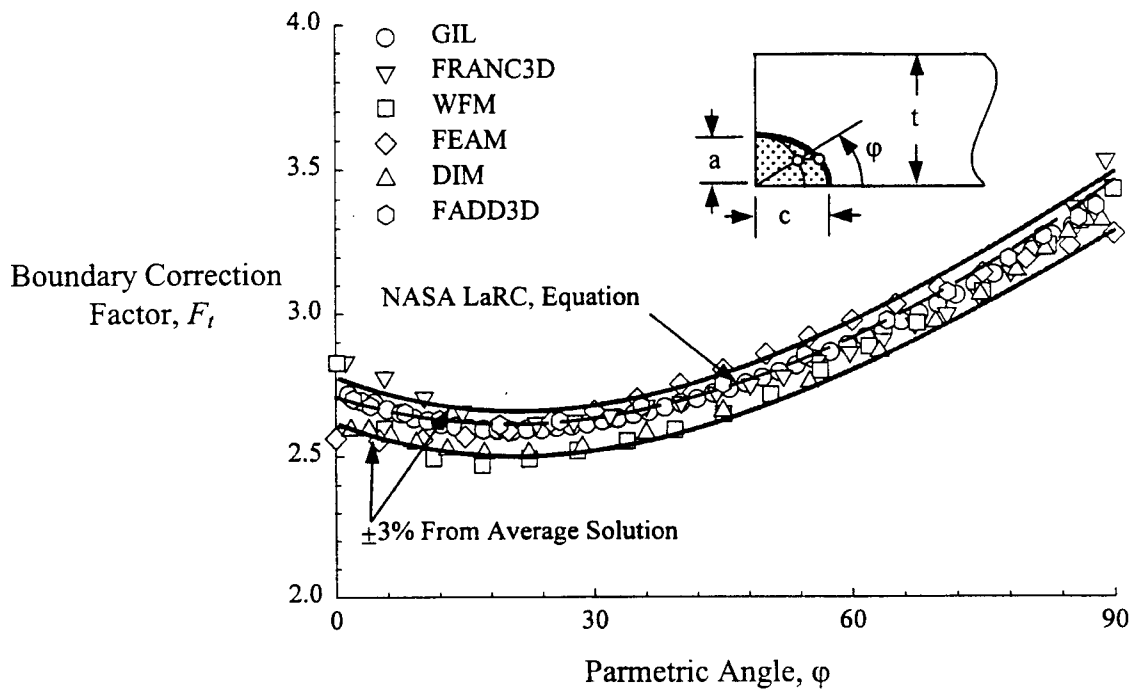


FIGURE 5. COMPARISON OF RESULTS FROM ALL SOLUTION METHODS

TABLE 1. STUDY PARTICIPANTS AND METHODS USED

Principle Investigator	Affiliation	Method
James Newman [26 ]	NASA Langley Research Center (LaRC)	Semiempirical SIF Equation
Paul Wawrzynek	Cornell University (CU)	The FRacture ANalysis Code in 3 Dimensions (FRANC3D)
Wei Zhao	University of South Carolina (USC)	Three-Dimensional Weight Function Method (WFM)
Daniel S. Pipkins	Knowledge Systems Incorporated (KSI)	Finite Element Alternating Method (FEAM)
Brian Moran [7]	Northwestern University (NWU)	Domain Integral Method (DIM)
Mark Mear	University of Texas, Austin (UTA)	Fracture Analysis by Distributed Dislocations in 3 Dimensions (FADD3D)
John Bakuckas	FAA William J. Hughes Technical Center	Global-Intermediate-Local (GIL)

TABLE 2. BOUNDARY CORRECTION FACTORS FROM THREE MESHES OF  
LOCAL MODEL

Mesh A – Conv.		Mesh B – Conv.		Mesh C – Sing.	
$\phi$	$F_t$	$\phi$	$F_t$	$\phi$	$F_t$
3.008	2.740	1.464	2.741	1.464	2.713
6.011	2.669	2.928	2.679	2.928	2.690
9.185	2.660	4.434	2.696	4.434	2.683
12.344	2.637	5.940	2.670	5.940	2.660
15.672	2.621	7.490	2.656	7.490	2.647
18.975	2.622	9.036	2.641	9.036	2.629
22.436	2.617	10.625	2.630	10.625	2.621
25.866	2.633	12.211	2.621	12.211	2.609
29.452	2.640	13.841	2.611	13.841	2.601
32.985	2.666	15.465	2.607	15.465	2.594
36.692	2.686	17.129	2.601	17.129	2.591
40.337	2.718	18.782	2.602	18.782	2.590
44.157	2.750	20.485	2.597	20.485	2.586
47.909	2.790	22.176	2.604	22.176	2.592
51.837	2.829	23.912	2.602	23.912	2.591
55.713	2.879	25.645	2.611	25.645	2.599
59.760	2.925	27.408	2.614	27.408	2.603
63.769	2.984	29.166	2.623	29.166	2.610
67.970	3.040	30.963	2.631	30.963	2.620
72.122	3.108	32.751	2.641	32.751	2.628
76.495	3.185	34.574	2.653	34.574	2.641
80.837	3.248	36.386	2.665	36.386	2.651
85.427	3.377	38.241	2.678	38.241	2.666
		40.082	2.696	40.082	2.681
		41.973	2.708	41.973	2.696
		43.847	2.731	43.847	2.715
		45.756	2.744	45.756	2.731
		47.658	2.766	47.658	2.750
		49.611	2.784	49.611	2.770
		51.535	2.806	51.535	2.790
		53.517	2.827	53.517	2.813
		55.477	2.852	55.477	2.836
		57.492	2.875	57.492	2.860
		59.486	2.901	59.486	2.885
		61.531	2.926	61.531	2.912
		63.573	2.955	63.573	2.937
		65.656	2.984	65.656	2.969
		67.728	3.015	67.728	2.997
		69.858	3.046	69.858	3.030
		71.970	3.081	71.970	3.062
		74.150	3.115	74.150	3.100
		76.314	3.155	76.314	3.136
		78.532	3.195	78.532	3.179
		80.755	3.238	80.755	3.220
		83.037	3.291	83.037	3.273
		85.314	3.310	85.314	3.302
		87.655	3.397	87.655	3.382

TABLE 3. BOUNDARY CORRECTION FACTORS FROM A VARIETY OF APPROACHES

FRANC3D CU		WFM USC		FEAM KSI		DIM NWU		FADD3D UTA	
$\phi$	$F_t$	$\phi$	$F_t$	$\phi$	$F_t$	$\phi$	$F_t$	$\phi$	$F_t$
1.125	2.830	0.125	2.826	0.000	2.561	1.737	2.592	2.000	2.697
5.619	2.774	5.619	2.594	5.000	2.554	3.810	2.592	4.000	2.673
10.211	2.703	11.322	2.493	10.000	2.556	6.303	2.570	8.000	2.649
14.635	2.653	16.947	2.470	15.000	2.567	9.308	2.545	12.000	2.625
18.999	2.604	22.460	2.492	20.000	2.588	12.897	2.524	19.000	2.608
23.288	2.613	28.065	2.518	25.000	2.619	17.213	2.511	26.000	2.620
27.604	2.619	33.832	2.552	30.000	2.654	22.389	2.511	35.500	2.670
31.820	2.638	39.389	2.590	35.000	2.697	28.605	2.531	45.000	2.749
36.037	2.672	45.041	2.644	40.000	2.748	36.058	2.578	54.500	2.850
40.135	2.683	50.557	2.712	45.000	2.800	45.000	2.654	64.000	2.972
44.219	2.717	56.315	2.796	50.000	2.855	55.080	2.755	71.000	3.073
48.179	2.746	61.919	2.882	55.000	2.914	63.146	2.864	78.000	3.192
52.021	2.776	67.477	2.964	60.000	2.973	69.602	2.968	82.000	3.271
55.939	2.828	75.015	3.075	65.000	3.030	74.765	3.064	86.000	3.335
59.742	2.860	82.536	3.240	70.000	3.088	78.891	3.150	88.000	3.374
63.529	2.905	86.237	3.324	75.000	3.141	82.197	3.224		
67.217	2.961	89.920	3.433	80.000	3.191	84.840	3.283		
70.905	2.996			85.000	3.238	86.950	3.324		
74.599	3.061			90.000	3.279	88.648	3.324		
78.229	3.145								
81.890	3.242								
85.515	3.372								
89.120	3.533								



TABLE 4. PARAMETERS USED IN SEMIEMPERICAL EQUATION [26]

Para.	$a/c \leq 1$	$a/c > 1$
$M_1$	$1.13 - 0.09\left(\frac{a}{c}\right)$	$\sqrt{\frac{c}{a}}\left(1 + 0.04\frac{c}{a}\right)$
$M_2$	$-0.54 + \frac{0.89}{0.2 + \frac{a}{c}}$	$0.2\left(\frac{c}{a}\right)^4$
$M_3$	$0.5 - \frac{1}{0.65 + \frac{a}{c}} + 14\left(1 - \frac{a}{c}\right)^{24}$	$-0.11\left(\frac{c}{a}\right)^4$
$g_1$	$1 + \left[0.1 + 0.35\left(\frac{a}{t}\right)^2\right](1 - \sin\varphi)^2$	$1 + \left[0.1 + 0.35\left(\frac{c}{a}\right)\left(\frac{a}{t}\right)^2\right](1 - \sin\varphi)^2$
$g_2$	$\frac{1 + 0.358\lambda + 1.425\lambda^2 - 1.578\lambda^3 + 2.156\lambda^4}{1 + 0.13\lambda^2}$	$\frac{1 + 0.358\lambda + 1.425\lambda^2 - 1.578\lambda^3 + 2.156\lambda^4}{1 + 0.13\lambda^2}$
$g_3$	$\left(1 + 0.04\frac{a}{c}\right)\left(1 + 0.1(1 - \cos\varphi)^2\right)\left[0.85 + 0.15\left(\frac{a}{t}\right)^{0.25}\right]$	$\left(1.13 + 0.09\frac{c}{a}\right)\left(1 + 0.1(1 - \cos\varphi)^2\right)\left[0.85 + 0.15\left(\frac{a}{t}\right)^{0.25}\right]$
$g_4$	$1 - 0.7\left(1 - \frac{a}{t}\right)\left(\frac{a}{c} - 0.2\right)\left(1 - \frac{a}{c}\right)$	$1$
$f_\varphi$	$\left[\left(\frac{c}{a}\right)^2 \sin^2\varphi + \cos^2\varphi\right]^{0.25}$	$\left[\left(\frac{c}{a}\right)^2 \sin^2\varphi + \cos^2\varphi\right]^{0.25}$
$f_w$	$\left[\sec\left(\frac{\pi R}{2W}\right)\sec\left(\frac{\pi(2R+2c)}{4(W-c)+4c}\sqrt{\frac{a}{t}}\right)\right]^{0.5}$	$\left[\sec\left(\frac{\pi R}{2W}\right)\sec\left(\frac{\pi(2R+2c)}{4(W-c)+4c}\sqrt{\frac{a}{t}}\right)\right]^{0.5}$
$\lambda$	$\frac{1}{1 + \frac{c}{R}\cos(0.85\varphi)}$	$\frac{1}{1 + \frac{c}{R}\cos(0.85\varphi)}$

